Electronic supplementary information

Continuous Production of Bimetallic Nanoparticles on Carbon Nanotubes Based on 3D-Printed Microfluidics

Bo Liu,[a,b] Jing Jin,*[b] Bin Ran,[b] Chaozhan Chen,[b] Jiaqian Li[a], Ning Qin[a] and Yonggang Zhu*[b]

[a] School of Energy and Power Engineering, Shandong University, Jinan, 250061, China

[b] School of Mechanical Engineering and Automation, Harbin Institute of Technology, Shenzhen, Shenzhen 518055, China

*Corresponding authors. E-mail: jinjing2020@hit.edu.cn (J. Jin), zhuyonggang@hit.edu.cn (Y. Zhu)

Contents

1. Tensile test specimen of 3D printed material

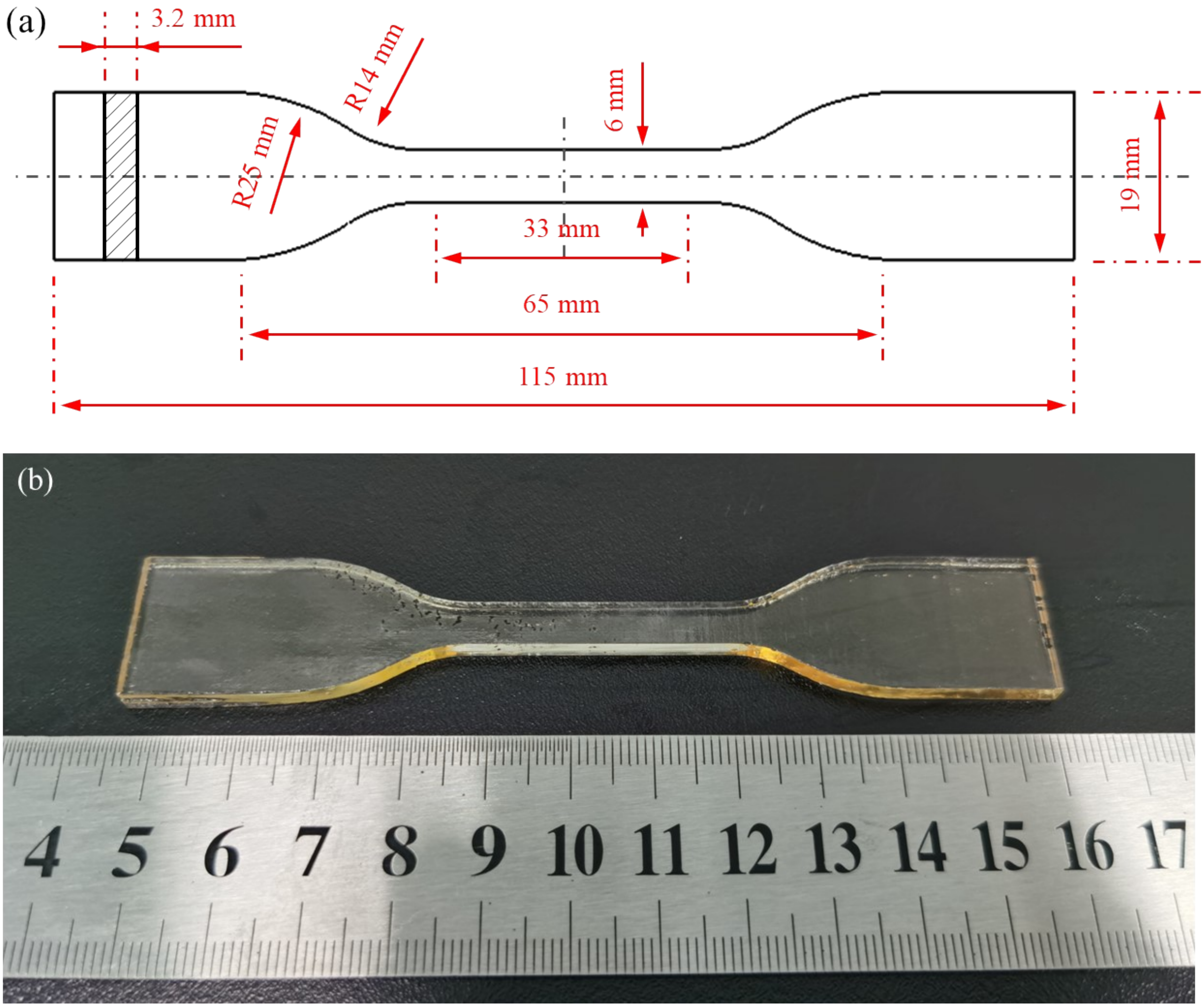

Fig. S1 Tensile test specimen of 3D printed material. (a) Dimensions of the tensile test specimen; (b) 3D printed specimen for the tensile test.

2. Microfluidic synthesis conditions for MWCNTs/Pt-Pd

Table S1 Microfluidic synthesis conditions for MWCNTs/Pt-Pd.

Item	Flow rate ratio of precursor (Q_A:Q_B)	Flow rate ratio of micromixer I (Q_{A+B}:Q_C)	Reduction concentration ratio (C_E:C_C)	Total flow rate (mL min^{-1})
TFR: 1	1:1	1:1	4	1
TFR: 5	1:1	1:1	4	5
TFR: 10	1:1	1:1	4	10
TFR: 15	1:1	1:1	4	15
PFRR:0.1	1:1	1:9	4	5
PFRR:0.3	1:1	3:7	4	5
PFRR:0.5	1:1	1:1	4	5
PFRR:0.7	1:1	7:3	4	5
PFRR:0.9	1:1	9:1	4	5
Pt-FRR: 0	0:1	1:1	4	5
Pt-FRR: 0.3	3:7	1:1	4	5
Pt-FRR: 0.5	1:1	1:1	4	5
Pt-FRR: 0.7	7:3	1:1	4	5
Pt-FRR: 1	1:0	1:1	4	5

3. Stress-strain curve of tensile test for 3D printed material

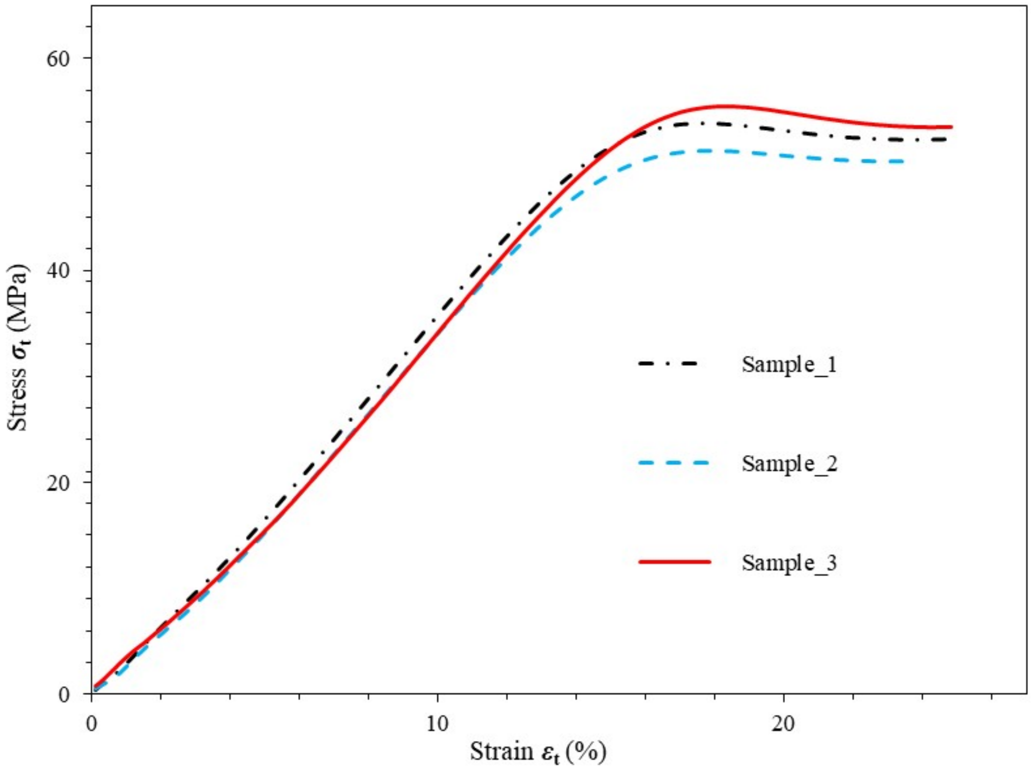

Fig. S2 Stress-strain curve of tensile test for 3D printed material.

4. 3D printing workflow of design and fabrication for 3D micromixer

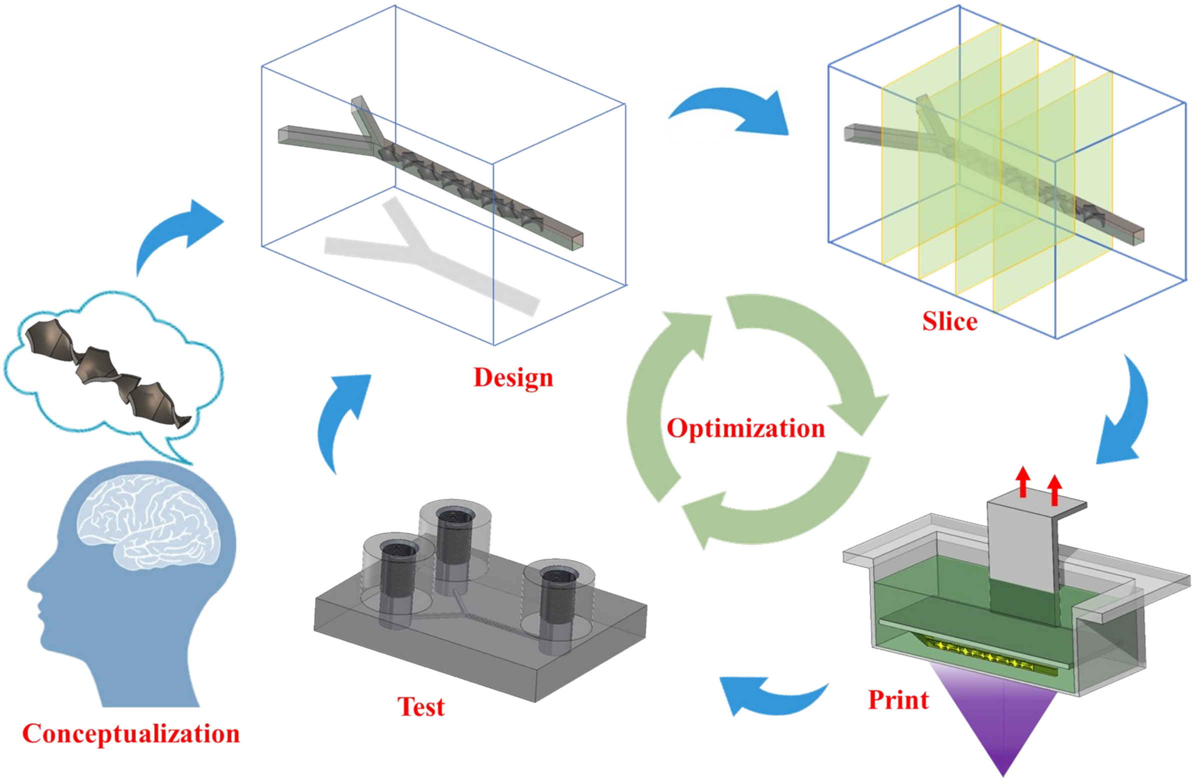

Fig. S3 3D printing workflow of design and fabrication for 3D micromixer.

5. Micro-CT scan of the micromixer I

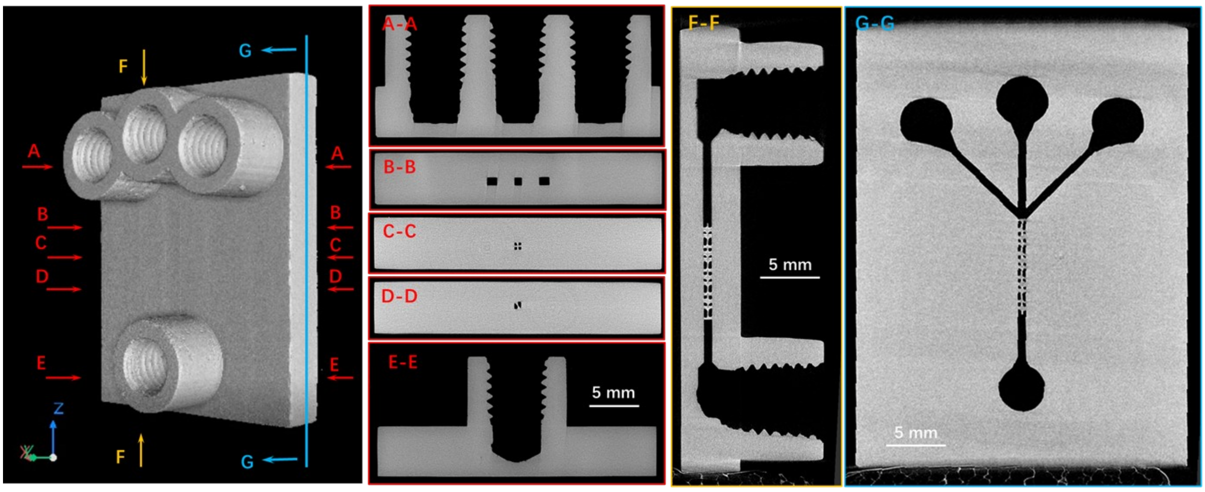

Fig. S4 Micro-CT scan of the micromixer I with different cross-sections.

6. Mixing performance of micromixer I

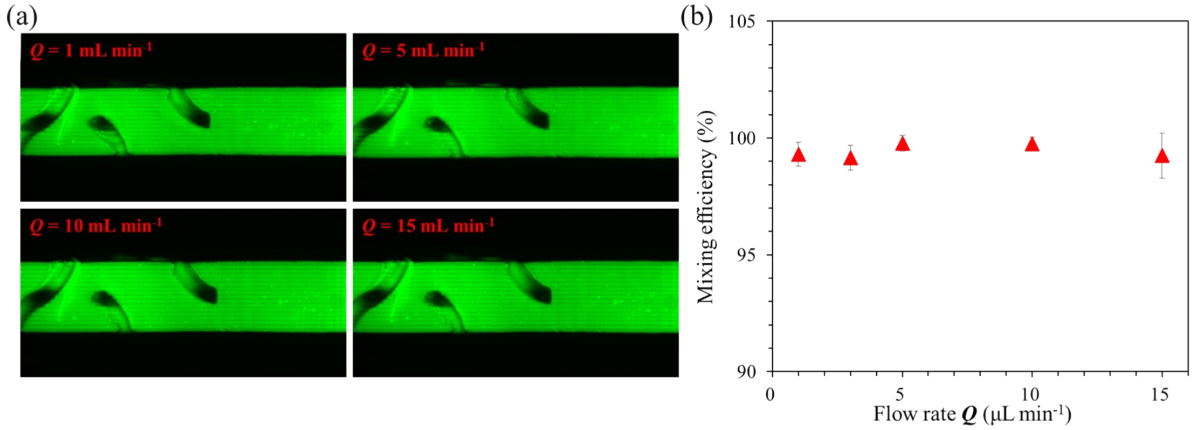

Fig. S5 Mixing performance of micromixer I. (a) Mixing efficiency of micromixer I with different flow rates; (b) The microscope fluorescein images at the outlet of micromixer I with different flow rates.

7. Comparison of synthesis throughout for nanoparticles

Table S2 Comparison of synthesis throughout for nanoparticles between different micromixers/microreactors.

Type	Fabricated material	Flow rate (mL min^{-1})	Synthesized material	Ref.
Y-shaped micromixer	PDMS	0.05~2	Ag NPs	[1]
T-shaped microreactor	PDMS	0.1	SnS NPs	[2]
Cross-shaped micromixer	PTFE	1	Pt/TiO_2	[3]
Cross-type mixer	PTFE	0.5~1.5	Ag/rGO	[4]
Spiral microreactor	PDMS	0.035~0.35	MNPs@ SiO_2	[5]
Spiral microreactor	PDMS	0.1~0.53	ZnO NPs	[6]
Droplet reactor	PDMS	0.008~0.02	SiO_2 NPs	[7]
Active microreactor	PDMS	0.1~0.5	Chitosan NPs	[8]
T-shaped micromixer	PDMS	1.5	Ag_2S NPs	[9]
Y-shaped micromixer	PDMS	0.17~1.7	Fe_3O_4 NPs	[10]
Droplet reactor	PDMS	~0.14	Au NPs	[11]
Y-shaped micromixer	PEEK	~0.15	CuS NPs	[12]
Droplet reactor	PDMS	0.01~0.025	TiO_2 NPs	[13]
Focusing microreactor	PDMS	0.01~0.013	Organic NPs	[14]
T-shaped micromixer	PTFE	0.7	MOF capsule	[15]
Acoustic micromixer	PDMS	0.01~0.05	Budesonide NPs	[16]
3D micromixer	Resin	1~15	MWCNTs/Pt-Pd	This study

8. TEM images of MWCNTs/Pd-Pt at different precursor flow rate ratios

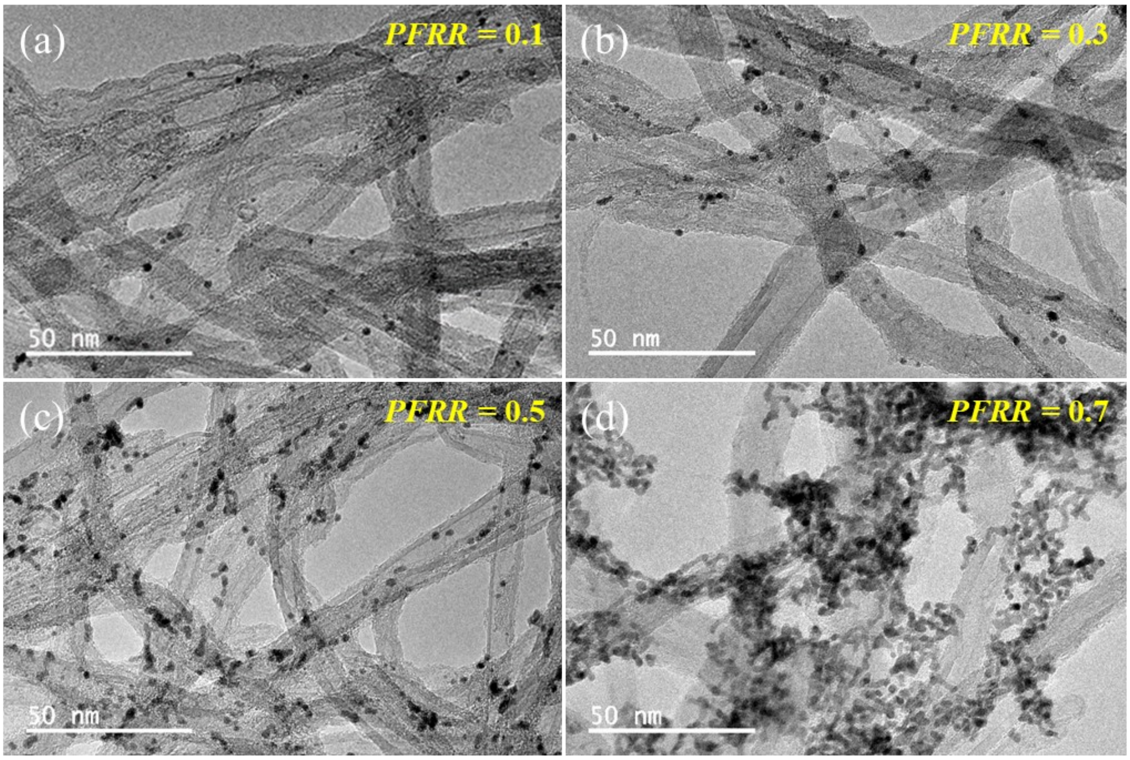

Fig. S6 TEM images of MWCNTs/Pd-Pt at different precursor flow rate ratios (*PFRR*), (a) 0.1, (b) 0.3, (c) 0.5, and (d) 0.7.

9. TEM images of MWCNTs/Pd-Pt at different Pt^{4+} flow rate ratios

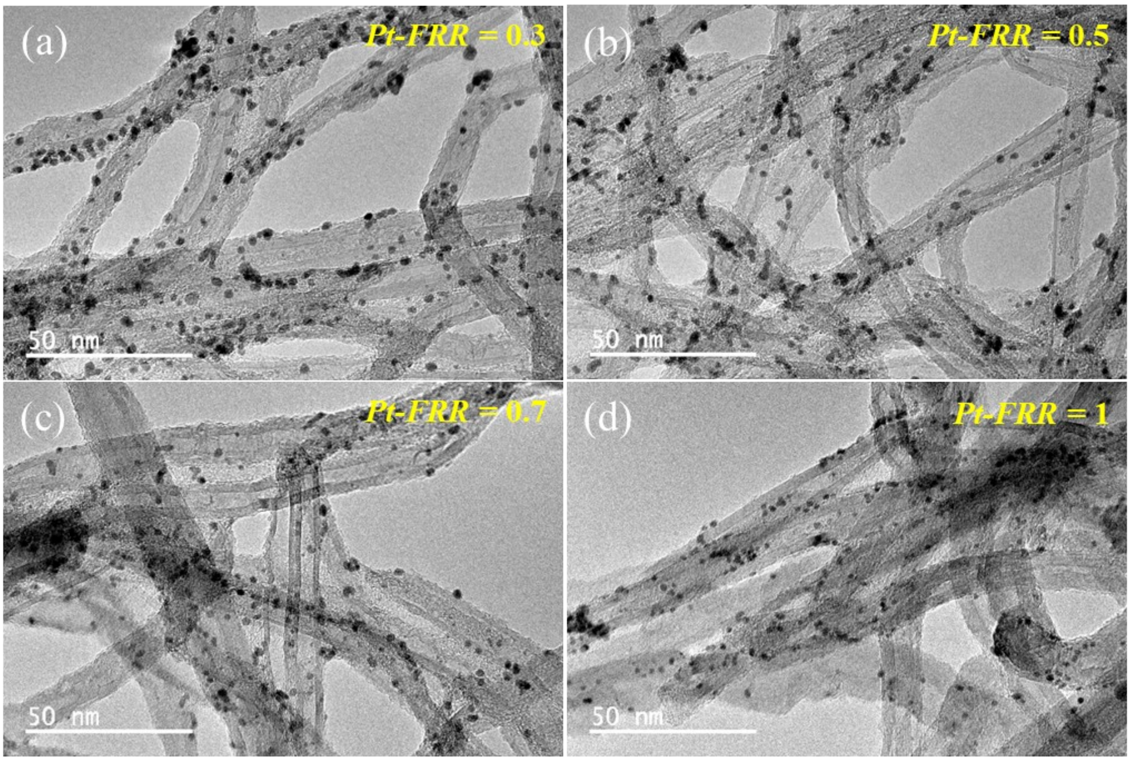

Fig. S7 TEM images of MWCNTs/Pd-Pt at different Pt^{4+} flow rate ratios (*Pt-FRR*), (a) 0.3, (b) 0.5, (c) 0.7, and (d) 1.

10. Comparison of current responses between modified electrodes

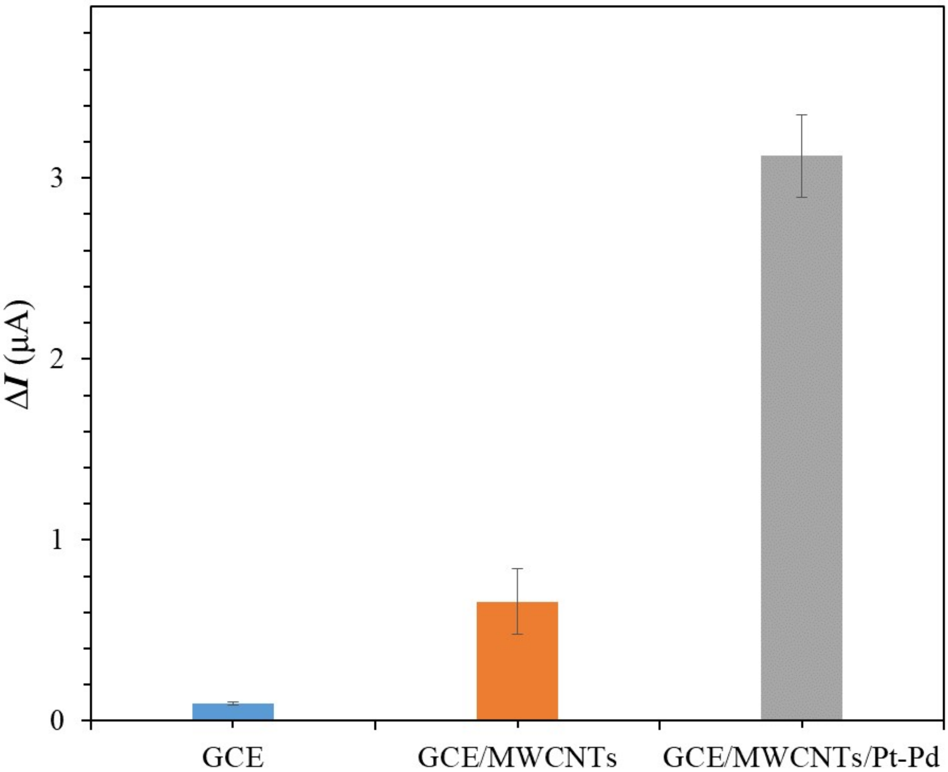

Fig. S8 Comparison of current responses of GCE, GCE/MWCNTs and GCE/MWCNTs/Pt-Pd under the optimized conditions.

11. Reproducibility of GCE/MWCNTs/Pt-Pd

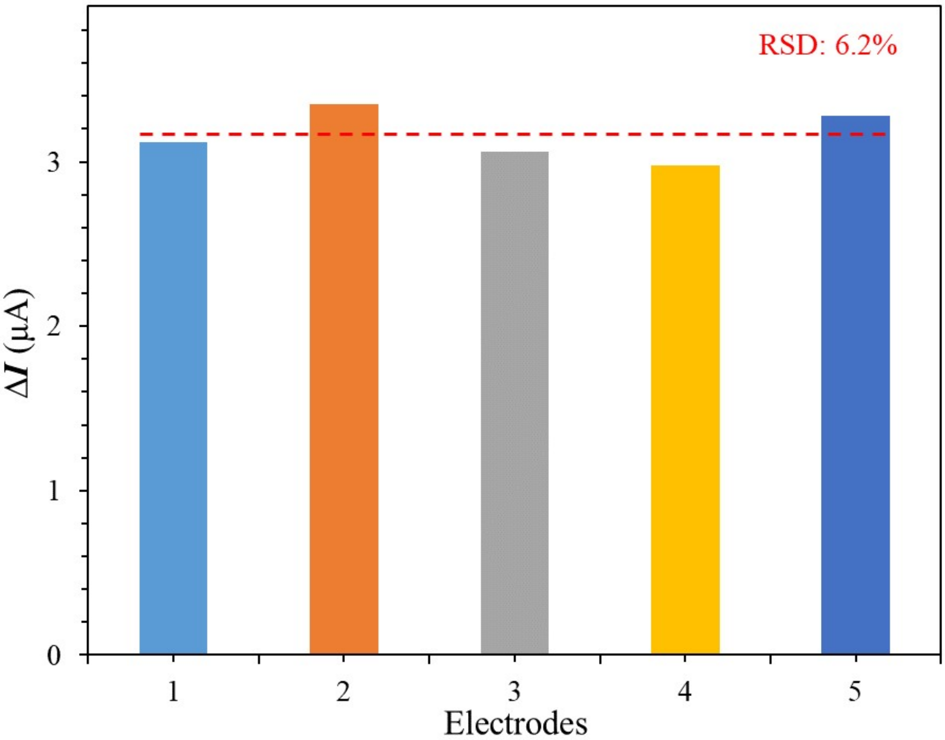

Fig. S9 Current responses of five different GCE/MWCNTs/Pt-Pd to 100 μM H_2O_2 in 0.1 M PBS (pH 7.4).

12. Reference

[1] Z. Yang, L. Dong, M. Wang, Y. Jia, C. Wang, P. Li, G. Liu, *Sensors and Actuators a-Physical* **2022**, 346.

[2] V. Katoch, M. Singh, A. Katoch, B. Prakash, *Materials Letters* **2023**, 333.

[3] L. Luo, M. Yang, G. Chen, *Chemical Engineering Science* **2022**, 251.

[4] S. Tao, M. Yang, H. Chen, G. Chen, *Acs Sustainable Chemistry & Engineering* **2018**, 6, 8719.

[5] N. Hao, Y. Nie, T. Shen, J. X. J. Zhang, *Lab on a Chip* **2018**, 18, 1997.

[6] N. Hao, Z. Xu, Y. Nie, C. Jin, A. B. Closson, M. Zhang, J. X. J. Zhang, *Chemical Engineering Journal* **2019**, 378.

[7] R. S. Pessoa, H. S. Maciel, G. Petraconi, M. Massi, A. S. da Silva Sobrinho, *Applied Surface Science* **2008**, 255, 749.

[8] V. Kamat, I. Marathe, V. Ghormade, D. Bodas, K. Paknikar, *Acs Applied Materials & Interfaces* **2015**, 7, 22839.

[9] B. Prakash, V. Katoch, A. Shah, M. Sharma, M. M. Devi, J. J. Panda, J. Sharma, A. K. Ganguli, *Photochemistry and Photobiology* **2020**, 96, 1273.

[10] T. Vu Thi, M. An Ngoc, T. Le The, T. Hoang Van, T. Phung Thi, T. Bui Quang, T. Nguyen Tran, L. Tran Dai, *Journal of Electronic Materials* **2016**, 45, 2576.

[11] S. Abalde-Cela, P. Taladriz-Blanco, M. G. de Oliveira, C. Abell, *Scientific Reports* **2018**, 8.

[12] I. Ortiz de Solorzano, M. Prieto, G. Mendoza, T. Alejo, S. Irusta, V. Sebastian, M. Arruebo, *Acs Applied Materials & Interfaces* **2016**, 8, 21545.

[13] P. Stolzenburg, T. Lorenz, A. Dietzel, G. Garnweitner, *Chemical Engineering Science* **2018**, 191, 500.

[14] V. Genot, S. Desportes, C. Croushore, J.-P. Lefevre, R. B. Pansu, J. A. Delaire, P. R. von Rohr, *Chemical Engineering Journal* **2010**, 161, 234.

[15] R. Ameloot, F. Vermoortele, W. Vanhove, M. B. J. Roeffaers, B. F. Sels, D. E. De Vos, *Nature Chemistry* **2011**, 3, 382.

[16] L. Nguyen Hoai An, P. Hoang Van, J. Yu, H.-K. Chan, A. Neild, T. Alan, *International Journal of Nanomedicine* **2018**, 13, 1353.